

See discussions, stats, and author profiles for this publication at: <https://www.researchgate.net/publication/44569076>

# Structural Responses of DNA–DDAB Films to Varying Hydration and Temperature

ARTICLE *in* JOURNAL OF THE AMERICAN CHEMICAL SOCIETY · MAY 2010

Impact Factor: 12.11 · DOI: 10.1021/ja909514j · Source: PubMed

---

CITATIONS

16

---

READS

23

5 AUTHORS, INCLUDING:



[Luc Jaeger](#)

University of California, Santa Barbara

95 PUBLICATIONS 3,218 CITATIONS

[SEE PROFILE](#)



[Matthew Tirrell](#)

University of Chicago

465 PUBLICATIONS 12,397 CITATIONS

[SEE PROFILE](#)

Published in final edited form as:

*J Am Chem Soc.* 2010 May 26; 132(20): 7025–7037. doi:10.1021/ja909514j.

## Structural responses of DNA-DDAB films to varying hydration and temperature

Thorsten Neumann<sup>1,3</sup>, Surekha Gajria<sup>2</sup>, Nathan F. Boussein<sup>1</sup>, Luc Jaeger<sup>2</sup>, and Matthew Tirrell<sup>1,\*</sup>

<sup>1</sup> Materials Research Laboratory, University of California, Santa Barbara, California 93106

<sup>2</sup> Department of Chemistry and Biochemistry, University of California, Santa Barbara, California, 93106

### Abstract

The structure of a DNA-dimethyldidodecylammonium bromide (DDAB) film was recently described to undergo a distinctive transition in response to the water content in the surrounding environment. 1 The existence, preparation, and basic properties of DNA-surfactant films have been known in the literature for some time. 2,3 Here, we describe the structural response of DNA-DDAB films to environmental changes, particularly temperature and humidity, in greater detail revealing new structural states. We can direct the lamellar structure of the film into three distinct states – double-stranded DNA (dsDNA) paired with an interdigitated bilayer of DDAB (bDDAB), single-stranded DNA (ssDNA) with monolayer of DDAB (mDDAB), and ssDNA with bDDAB. Both temperature and humidity cause the molecules composing the lamellar structure to change reversibly from ssDNA to dsDNA and/or from mDDAB to bDDAB. We found that the structural transition from dsDNA to ssDNA and bDDAB to mDDAB is concerted and follows apparent first order kinetics. We also found that the double-stranded conformation of DNA in the film can be stabilized with the inclusion of cholesterol even while the DDAB in the film is able to form either a monolayer or bilayer depending on the environmental conditions. Films treated with ethidium bromide prompt switching of dsDNA to ssDNA before bDDAB transitions to mDDAB. Swelling experiments have determined that there is a direct proportionality between the macroscopic increase in volume and the nanoscopic increase in lamellar spacing when a film is allowed to swell in water. Finally, experiments with phosphate-buffered saline (PBS) indicate that the films can disassemble in a simulated biological environment due to screening of their charges by buffer salt. We conclude that the structure of DNA in the film depends on the water content (as measured by the relative humidity) and temperature of the environment, while the state of DDAB depends essentially only on the water content. The structure of the film is quite flexible, and can be altered by changing environmental conditions as well as the chemical ingredients. These films will have useful, new applications as responsive materials, e.g. in drug and gene delivery.

### Keywords

nucleic acid-surfactant films; biomaterials; responsive materials; DNA

\*To whom correspondence should be addressed. mvtirrell@berkeley.edu.

<sup>3</sup>Current address: Department of Bioengineering, University of California, Berkeley, California, 94720

### Supporting Information

Additional information available regarding the characterization of the structure and physical behavior of the films under various conditions. This material is available free of charge via the Internet at <http://pubs.acs.org>.

## Introduction

It is well-known that naturally derived polyanions such as nucleic acids (RNA and DNA) can self-assemble with cationic lipids or surfactants via electrostatic attractions, thermodynamically driven by the release of counterions.<sup>4</sup> Applications of these types of complexes are frequently used in the fields of gene and siRNA delivery.<sup>5</sup> Most of these complexes are dispersed in aqueous solution with well understood and characterized structures.<sup>5-6,7,8</sup> It has been found that the complex structure (such as lamellar or inverted hexagonal) is mainly dependent on the lipid used for complexation.<sup>9,10</sup> However, little is known about the behavior of the complexes in the dry state, particular in the physical state of a macroscopic film. Dry films or coatings may have distinct advantages for drug or nucleic acid delivery such as direct implantation at the site of interest, greater storage capabilities, ease of handling, etc.

The simple preparation of solid self-standing DNA-cationic surfactant films was previously reported by Okahata et al.,<sup>2,3</sup> and was adopted by our group with slight modifications (see Materials and Methods). The films obtained have certain interesting features such as controllable mechanical properties, which vary with the type and amount of nucleic acid (NA) used.<sup>11</sup> Our studies focus on complexes with the surfactant dimethyldidodecylammonium bromide (DDAB), which tend to form stable lamellar bilayers independent of the surrounding temperature for concentrations greater than 3%,<sup>12,13</sup> which was also confirmed by a harmonic series of peaks in our scattering data (Table S1 and Figure S1).

We assume that the electrostatic coupling parameter between negatively charged DNA and positively charged DDAB is  $\Xi \gg 1$  and in the range of  $10^2$ , comparable to the strong DNA-spermidine binding described in the literature.<sup>14</sup> This is because DNA and DDAB arrange as 2D layers in the film which does not dissolve into free ions when immersed in water.

In a recent publication, we gave detailed structures of a DNA-DDAB film in wet and dry states showing that the DNA switches from being single stranded (ssDNA) to double stranded (dsDNA) while the cationic amphiphile DDAB undergoes a transition from a monolayer (mDDAB) to an interdigitated bilayer (bDDAB).<sup>1</sup> We found that the preferred state of DNA and DDAB in the film is highly dependent on the surrounding environment; particularly the water content. In the hydrated state the nucleic acid and surfactant prefer the dsDNA-bDDAB formation while in the dry state the ssDNA-mDDAB formation is preferred.

Such a unique structural change prompts further investigation into its cause and the extent to which it can be manipulated. No extensive studies have been done to date with DDAB or for nucleic acid-lipid complexes in the solid state and to our knowledge no switching behavior as a function of water content such as we have seen for our films has been reported in the literature. Such a structural change occurring upon hydration of the film could be used to manipulate the film into “on” and “off” states; i.e. when the film is dry it is biochemically inactive or “off”, and when hydrated (for example during implantation in a patient) it is able to change its structure, possibly presenting therapeutic nucleic acids, peptides or small molecules for release *in vivo* as the film degrades.

In order to better understand these phenomena, we determined the level of humidity needed to induce the switching, the reversibility and stability of this process, the speed of the transition, and other induced structural transitions of the films due to various environmental stimuli (such as temperature) and chemical additives (such as cholesterol and ethidium bromide), which to our knowledge have not been reported for similar materials. Such processes are important to understand for the application of the films as drug delivery devices, in which they may be loaded with therapeutic small molecules, which would interact with the film differently in the dry state than in the wet.

As we wish to develop the application of these films for the controlled release of drugs either by blending them into the film or binding to (or intercalating into) the nucleic acid we are particularly interested in how a film would break down in a simulated biological environment, for example by monitoring the film response to an aqueous phosphate buffer.

## Materials and Methods

### Nucleic acid and solvents

DNA from salmon testes sperm (2,000 base-pairs long, as determined by agarose gel electrophoresis) purchased from Sigma-Aldrich was used in these studies to form complexes with the quaternary cationic surfactant DDAB purchased from TCI America. All materials were certified as DNase free. The TBE 1X buffer (89 mM Trisborate, 0.2 mM EDTA) used in this study was prepared from 10X TBE buffer (Omnipur brand purchased from EMD Chemicals) and ultra pure water (Milli-Q). Isopropanol was purchased from Merck and used after filtration with a 0.45  $\mu\text{m}$  filter. Ethidium bromide (stock solution 10 mg/ml) purchased from Sigma was used for the intercalation experiments. Cholesterol was purchased from USB Corporation.

### Film preparation

Films were prepared as described previously<sup>1</sup>: 100 mg DNA dissolved in TBE 1x buffer was mixed with a solution of 161 mg DDAB (1.1 eq) in water. After shaking for 3 hours, the complexes were purified, dried and dissolved in isopropanol. Unless otherwise noted the films were cast from 1 mL of a 20 mg/mL complex solution onto glass or silicon slides (18  $\times$  18 mm) and allowed to dry under ambient conditions in air. The complexation was complete after 3 hours according to small-angle X-ray (SAXS) experiments (Figure S2).

For the ethidium bromide intercalation experiments, the procedure was modified in that the aqueous DNA solution was treated with a specific amount of ethidium bromide and incubated for an hour, followed by mixing with the DDAB solution. The resulting complex was also washed three times before it drying under vacuum. The amount of ethidium bromide intercalated in the DNA of the complex was determined by subtracting the amount of unbound ethidium bromide in the supernatant as measured UV-Vis spectroscopy at absorption of 595 nm from the total amount added (Figures S14 and S15). The percentage of ethidium bromide added was based on the total number of base-pairs it could intercalate. The cholesterol-modified DNA-DDAB films were prepared from a mixture of DNA-DDAB complex and cholesterol dissolved in isopropanol followed by casting on glass slides. The percentage of cholesterol added was based on weight.

### FT-IR measurements

Fourier-transform infrared spectroscopy measurements were performed by a Nicolet Magna 850 IR/Raman spectrometer. The films were cast on double-sided polished silicon substrates from a solution of 20 mg/mL DNA-DDAB complex in isopropanol, unless otherwise noted. A blank silicon substrate was used to measure the background spectrum. The spectra were measured from 400  $\text{cm}^{-1}$  to 4000  $\text{cm}^{-1}$  under a constant flow of nitrogen of 40 sccm. For each spectrum eight scans were averaged. For the structural switching analysis the film, which was still attached on the silicon substrate, was immersed in water for five minutes or else 100–200  $\mu\text{L}$  of water was added on top of the film in the sample chamber after the first two scans, as noted in the text. These films are designated as water-immersed or wetted, respectively. Various water immersion times between five seconds and five minutes were also measured and no significant differences in transition speed were observed either between films immersed for different periods of time or between wetted and water-immersed films (Figure S5). Excessive water was removed before the film was placed in the spectrometer. Within the FT-IR chamber

a lowered constant flow of nitrogen (20–30 sccm) allowed the film to dry slowly. During the drying process FT-IR spectra were taken continuously and every ten seconds for 20 minutes. For the quantitative analysis of DNA structural switching the absorption bands at 1695 and 1653  $\text{cm}^{-1}$  were used while the bands at 2850, 2925 and 2968  $\text{cm}^{-1}$  were used for the DDAB structural switching analysis. Both sets of peaks were fitted by Origin (Originlab). The ratio of the integrated signal was taken from the peak intensities at 1695 to 1653  $\text{cm}^{-1}$  for the DNA and 2925 to 2968  $\text{cm}^{-1}$  for the DDAB band. The absorption band at 1650  $\text{cm}^{-1}$  decreased steadily while the band at 1690  $\text{cm}^{-1}$  stayed nearly constant in intensity as the wetted film dried. The area of both absorption bands were determined by integration of both peaks using a Lorentz profile. The results were plotted as a ratio of the area of 1650 to 1690  $\text{cm}^{-1}$  and 2925 to 2968  $\text{cm}^{-1}$ . All data were normalized in intensity for more effective analysis.

Constant humidity level FT-IR experiments were performed in a humidity chamber that was sealed with two silicon windows on each side, of which one was coated with a DNA-DDAB film. The humidity level inside the chamber was adjusted by placing various saturated salt solutions (same as used for the WAXS and SAXS experiments) in a reservoir in the chamber underneath the film such that the film had no contact with the salt solution. After 6 hours incubation time at one humidity level the film was measured between 400 and 4000  $\text{cm}^{-1}$ . Control experiments at 48 hours at certain humidity levels showed no difference from the 6 hour spectra. All data obtained from these measurements were normalized in intensity for more effective analysis.

### Small- and wide-angle X-ray scattering (SAXS and WAXS)

Transmission SAXS and WAXS measurements were performed with Cu K $\alpha$  radiation using a custom built X-ray diffractometer with MAR180 (SAXS) and MAR345 (WAXS) image plate detectors and a Rigaku (UltraX18HF) rotating anode X-ray generator. The sample to detector distance was 755.89 mm for SAXS and 235 mm for WAXS. The integrated diffraction data were plotted as a function of  $q=(4\pi/\lambda)\sin(\theta)$ , where  $\lambda$  is the wavelength of the beam ( $\lambda = 0.154$  nm) and  $\theta$  is the Bragg angle. The experimental data were corrected for background scattering and sample attenuation. Each film was cast either from 200  $\mu\text{L}$  of 5 mg/mL solution in isopropanol into a 1.5 mm quartz capillary tube purchased from Hampton Research Co. or on a solid substrate, as noted in the text. Due to the slow evaporation process under ambient conditions the solvent was removed under vacuum within two hours. No discernable difference in X-ray scattering was observed between films dried in vacuum and those dried under ambient conditions in air, as well as for films cast in capillaries and those cast on solid substrates like glass or silicon (data not shown). Films with added ethidium bromide or cholesterol were removed from their solid casting substrates (e.g. silicon) and taped to a sample block with double-sided tape before analysis.

The humidity measurements were performed on films which were prepared by casting the standard DNA-DDAB complex solution in isopropanol onto double-sided polished silicon substrates with dimensions of  $20 \times 10$  mm. The films were removed before analysis using a scalpel and tweezers. The films were mounted on a glass frame using double-sided tape which was placed inside a Falcon tube. The sides of the tube were cut out and replaced by Kapton (DuPont) foil to serve as a window. The humidity was adjusted by the following saturated salt solutions with particular relative humidity levels (R.H.) which were placed at the bottom of the Falcon tube: lithium chloride (11 % R.H.); potassium acetate (22% R.H.), magnesium chloride (33% R.H.), potassium carbonate (43 % R.H.), sodium bromide (60 % R.H.), sodium chloride (75 % R.H.), potassium chloride (88 % R.H.) and potassium sulfate (95 % R.H.).<sup>15, 16, 17</sup> All data were normalized in intensity for more effective analysis. Equilibrium humidity between the surrounding environment and the film in each chamber was assumed after 6 hours

as no discernable difference in X-ray scattering spectra was observed between films left to equilibrate for 3 hours and those left to equilibrate overnight (data not shown).

For the temperature SAXS experiments a home-built heating chamber was used which was heated by a Peltier element and controlled by an Omega RS-100 temperature controller with a Kapton low voltage meter. The chamber windows were prepared with two layers of Kapton foil. The temperature was varied between 25 °C and 90 °C. Each sample was annealed at a certain temperature for 30 minutes before analysis. Both dry and wet films were measured in this setup. In order to prevent evaporation of water during heating for the wet film, the capillary was sealed with a Teflon cap. To ensure that samples were being measured at equilibrium, one film was held at 75 °C overnight (~16 hours) and then analyzed by SAXS. As no discernable difference was observed between this sample and those left to equilibrate for 30 minutes (Figure S10) we assume that scattering data of all the temperature-modified films were measured in an equilibrium state.

Synchrotron X-ray experiments were carried out at the Stanford Synchrotron Radiation Laboratory beam-line BL4-2 at 9 keV with a 20 pole 2.0 tesla wiggler. A Rayonix MX225-HE 2D area detector (Evanston, IL) was used to collect the scattering patterns. Sample to detector distance was 1.2 meters and silver behenate was used as a standard to calibrate the momentum transfer ( $q$ ). The images were azimuthally integrated to give scattering intensity versus momentum transfer  $q$ . Films were prepared as described above for the humidity experiments with SAXS. Whether the films were cast and measured on a silicon substrate (FT-IR studies) or Kapton (synchrotron SAXS, data not shown) or measured without a substrate after being removed from the casting substrate (SAXS experiments) had little observed effect on the drying behavior.

### CD measurements

The CD measurements were performed on an OLIS RSM circular dichroism spectrometer with a 0.1 mm cuvette and a standard concentration of 1 mg/mL for native DNA in water and DNA-DDAB in isopropanol within the range of 200 nm to 350 nm. The dry film was prepared from a 10 mg/mL solution of DNA-DDAB complex in isopropanol which was cast inside a quartz glass cuvette (10 × 10 × 40 mm). Since the film was transparent we were able to measure CD spectra of the dry film. For each sample spectrum 70 data points at an integration time of 10 seconds were taken, averaged over two scans, and adjusted for the concentration and weight of DNA.

Temperature-resolved measurements of the dry DNA-DDAB film with the CD spectrometer were taken between 200 and 350 nm while the temperature was increased from 25 °C up to 100 °C in 5 °C steps. The temperature was allowed to equilibrate for two minutes between each step. The same measurements were performed when the film was immersed in water. In order to prevent evaporation of water the cuvette was sealed with a Teflon cap and Parafilm during the heating process. For the temperature measurements a background spectrum of the empty cuvette was taken and subtracted from the original data.

### Swelling experiments

For the macroscopic swelling experiments a thick DNA-DDAB film was cast stepwise from a solution of 260 mg DNA-DDAB complex in 13 mL isopropanol in a custom-made square-shaped glass mold with dimensions of 17 × 17 × 20 mm and dried under vacuum to remove all trapped solvent. The resulting dry film had the same weight (260 mg) as the initial amount of complex and a thickness of 900 μm. The film was then immersed in 50 mL of water. During the swelling procedure the increase in water retention was monitored every 30 seconds by removing the film from the water and weighing after removing all excess water. The swelling



process was complete after 150 seconds, as there was no further increase in weight. The dimensions of the fully swollen film increased in average over three runs from  $17 \times 17 \times 0.9$  mm to  $19 \times 19 \times 1.2$  mm which adds up to a cubic swelling rate of 155%. The weight of the film increased from 260 mg to 407 mg, the same percentage (155%) as the increase in volume.

### Disassembly studies

A typical DNA-DDAB film was cast as described above, immersed in a 1 mg/mL aqueous solution of ethidium bromide for 48 hours, and then dried in air. 10  $\mu$ L of 1x phosphate-buffered saline (PBS) buffer was added in one spot on top of the film to simulate conditions *in vivo* and allowed to dry under ambient conditions in air. The salt residue was washed from the film using Milli-Q water before further analysis. The resulting area was examined by white light and fluorescence microscopy using 520 and 610 nm filters and atomic force microscopy (AFM). The AFM analyses were performed by a BioMFP-3D stand-alone AFM from Asylum research. The images were recorded in tapping mode using moderate force ratio under ambient conditions with commercial silicon tips Olympus AC240TS with resonance frequency  $f = 70$  kHz and spring constant  $k = 2$  N/m. A typical scan range of 5  $\mu$ m with a resolution of  $512 \times 512$  pixels was used for each image. Each sample was analyzed in multiple regions. Raw data was leveled by a first and second order of plane fit correction in order to remove the sample tilt.

## Results and Discussion

### Cooperativity of the DNA and DDAB Switching Transitions in the Cast Film

Recently we reported the structural change of DNA-DDAB films triggered by the surrounding water content.<sup>1</sup> Interestingly, this transition was not observed for standard anionic polymer complexes, such as polystyrene sulfonic acid (PSSA)-DDAB films or polyacrylic acid (PAA)-DDAB films (Figure S3), thus highlighting the unusual behavior of DNA-DDAB complexes. The structural transition of the films was previously established by four methods: small-angle X-ray scattering (SAXS), Fourier transform infrared spectroscopy (FT-IR), circular dichroism (CD) spectroscopy, and fluorescence spectroscopy.<sup>1</sup>

In the FT-IR spectra the transition from dsDNA to ssDNA was monitored by the peaks at 1690  $\text{cm}^{-1}$  and 1650  $\text{cm}^{-1}$ , while the peaks at 2924 and 2966  $\text{cm}^{-1}$  were monitored for the switching from bDDAB to mDDAB (Figure S4, adapted from reference 1). Previously the complete transition profile of the film as a function of hydration from wet to dry based on the changes in FT-IR peak ratio was unknown as well as whether there was any cooperativity between the switching of DNA and DDAB. To this end the DNA-DDAB film was immersed in Milli-Q water and then slowly dried in the FT-IR spectrometer while spectra were taken every ten seconds (see Materials and Method). As most structural changes occurred in the first 400 seconds this range, as shown in Figure 1A, was used for further analysis. The decrease in DNA peak ratio indicating the transition of dsDNA to ssDNA can be clearly seen, indicated by the purple and green arrows in Figure S5A. A similar decrease in peak ratio can be observed in the DDAB tail region, marking its transition from bDDAB to mDDAB.<sup>18</sup> Peak ratios in both the DNA and DDAB regions increased immediately upon addition of water (Figure S6).

The averaged decrease in both DNA and DDAB peak ratio for a film wetted with 100–200  $\mu$ L of deionized water during the drying transition pathway can be fitted with an exponential curve (Figure 1A) assuming that the transition follows first order kinetics. The k-value of the resulted curve represents the apparent rate constant of the films' structural transition under the conditions described above and was measured to be  $0.014 \pm 0.002$  seconds<sup>-1</sup> (average of four independent experiments). A slightly higher k value for DNA ( $0.016 \pm 0.002$  seconds<sup>-1</sup>) compared to DDAB ( $0.012 \pm 0.002$  seconds<sup>-1</sup>) was found, which lies in the range of error and

is not discussed further. Interestingly these experiments were repeated up to four times (Figure S7) with the same results. No significant differences in transition speed could be found either between immersing the films for different periods of time in water or between wetting the films with water versus immersion in water, as the  $k$  values measured for each type are within 1.5% of each other on average (Supporting Information).

These results indicate that DNA and DDAB molecules undergo a structural transition together within the first 75 seconds as their  $k$  values are nearly identical (Figure 1A) and their peak ratios increase and decrease simultaneously upon addition of water (Supporting Information). We therefore propose that the switching of a DNA-DDAB film is cooperative. The initial scan after the casting of the film indicates that DNA switches shortly before DDAB the first time the film is wetted (Figure S6), but in the following cyclical scans the transition occurs simultaneously (Figure S7). It is of interest to note that the mDDAB peak ratio is comparatively lower after the first switching transition compared to the initial scan of the dry cast film, which suggests that portions of DDAB remain as bDDAB in the dried film due to retention of water within the bilayer. We also assume that isopropanol solubilizes DDAB more effectively and prevents high retention of water, increasing the mobility of DDAB and facilitating formation of mDDAB.

We further assume that the speed of the DNA denaturation to ssDNA and annealing back to dsDNA is due to the limited diffusion of DNA within the film, ensuring the ability to form the preferred wet or dry structural conformation in a relatively short amount of time, which was recently confirmed in DNA-lipid systems by NMR.<sup>19,20</sup> We believe that the DNA strands do not completely denature due to their long length, and therefore do not separate very far from each other as the film dries, making their renaturation faster than otherwise expected. These regions would then act like anchors, contributing to the relatively rapid and repeatable transition.

While initially surprising, the validity of our previous results on the switching of the films<sup>1</sup> was reinforced by reference to previous literature on the limited stability of the DNA helix in low water content hydrophobic solvents.<sup>21,22</sup> It is commonly known that an increase in temperature weakens the hydrogen bonds between the bases of DNA, resulting in melting (separation into two strands) above a certain threshold, depending on the length of the strand as well as the nature of the surrounding environment such as concentration of salt and hydrophobic molecules.<sup>21,23</sup> It is thought that a combination of electrostatic and hydrophobic effects is responsible for the unwinding and separation of DNA when exposed to hydrophobic solvents,<sup>21,24</sup> as the presence of these solvents destabilizes the favored base-stacking interactions which are most responsible for the stability of double-helical DNA in water.<sup>25</sup> Once the charges on DNA are effectively removed by electrostatic interaction with the DDAB headgroups and the environment becomes very hydrophobic by the loss of water, we believe that it is more thermodynamically favorable for the material to adopt the structure we have offered in the model, in which the hydrophobic DNA bases mix with the hydrophobic DDAB tails and the charged headgroups remain paired<sup>1</sup>.

Additionally, the number of alkyl groups in denaturing agents is known to affect the degree of DNA denaturation.<sup>26</sup> During hydration, the DDAB headgroup is surrounded by water, driving the lipid into a bilayer regime with highly interdigitated tails as indicated by the phase diagram of DDAB.<sup>27,28</sup> The hydration also presumably prompts the sequestering of the hydrophobic DNA bases by re-pairing of the double helix. It is not yet clear which event drives the other; however from our FT-IR data we conclude that the events are cooperative. Lipid bilayers weaken when dried, which can be observed in the increase in bilayer thickness and a lower degree of tail intercalation.<sup>29,30</sup> We assume that the lower degree of intercalation increases the chance of separating the bilayer into monolayers, driven by ionic forces (electrostatic



interactions with DNA). It is not possible that DDAB is in a liquid-crystalline ( $L_\alpha$ ) state and does not change upon interaction with DNA as its phase transition temperature (15–16 °C) is below room temperature.<sup>31</sup>

### Structural Reversibility using Humidity

The results obtained in our previous work confirm that the dry film has a lamellar spacing of 2.8 nm  $\pm$  0.2 nm which corresponds to mDDAB (1.7 nm)<sup>32</sup> in combination with ssDNA (1.1 nm).<sup>33</sup> When the film was immersed in water, the lamellar spacing increased to 4.3 nm  $\pm$  0.2 nm which corresponds to a fully interdigitated bilayer of DDAB (bDDAB, 2.4 nm)<sup>27,28</sup> in combination with dsDNA (2 nm). The fully interdigitated bilayer of DDAB is its most prevalent fraction according to the phase diagram<sup>27,28</sup>, so it is not unexpected that it would be also be common in the wet film.

Since environmental water content has a major influence on the structure of the film's components, we reasoned that it could also be altered by the relative humidity level (R.H.) of the film's environment and would provide more detailed knowledge of the amount of water needed to induce the switching. It is known from the literature that native DNA molecules are fully hydrated at a humidity level of 80% R.H., while higher humidity levels only increase the swelling of dsDNA.<sup>34,35</sup> Subsequently we investigated the structural changes that DNA undergoes during the drying process of the wet film as a function of R.H. (R.H. values are given in vapor pressures in Table S3). For these experiments the environmental humidity levels were adjusted between 11 % and 95% R.H. by the use of saturated salt solutions in a closed chamber.<sup>17</sup> When the DNA-DDAB films were exposed to low humidity levels (between 11 and 33% R.H.) the 1650  $\text{cm}^{-1}$  peak remained higher than the 1690  $\text{cm}^{-1}$  peak indicating that the DNA was single stranded and DDAB was arranged in a monolayer as measured before for a dry film (Figure 1B).<sup>1</sup> When the humidity increased the 1690  $\text{cm}^{-1}$  peak increased simultaneously, indicating a transition to dsDNA. A threshold humidity of ~60% R.H. was necessary to induce both the DNA transition of the film from ssDNA to dsDNA (Figure 1C) and for DDAB switching behavior from mDDAB to bDDAB (Figure S7).

To verify that the structural transition occurs at a threshold level of 60% R.H. and to correlate the FT-IR data to the lamellar spacing of DNA and DDAB molecules within the film, small-angle X-ray scattering (SAXS) measurements were performed using various relative humidity (R.H.) levels adjusted by salt solutions in a sealed chamber at equilibrium as described for the FT-IR experiments.<sup>17</sup> The scattering data of the film for each humidity level is shown in Figure S9A and the calculated lamellar spacing as a function of humidity level is shown in Figure 2A. Within the range measured the  $q$ -value in the films' X-ray scattering spectra decreases dramatically (increasing lamellar spacing) with increasing levels of R.H. At low R.H. between 10 and 40% the  $q$ -value of the main scattering peak lies in the range 2.1–2.2  $\text{nm}^{-1}$  which corresponds to a lamellar spacing of 2.8–3.0 nm. This distance can be reasonably assigned to ssDNA and mDDAB, typical of a dry film. The increased lamellar spacing at 5 % R.H. compared to the humidity level between 10 % and 45 % R.H. is similar to the phenomenon seen in lipid bilayers upon drying.<sup>29,30</sup> At 60% R.H. the transition process begins as indicated by a decrease in  $q$ -value to 2.0  $\text{nm}^{-1}$  and a corresponding lamellar spacing increase to 3.2 nm, similar to the increase in the DNA and DDAB peak ratio in the FT-IR data. At 75% R.H. the film  $q$ -value decreases further from 2.1 to 1.8  $\text{nm}^{-1}$  (an increase to 3.5 nm in the lamellar spacing) and reaches a maximum at 95 % R.H. with a lamellar spacing of 4.2 nm (0.1 nm less than compared to the lamellar spacing of a film immersed in water). The lamellar spacing increase triggered by relative humidity can be fitted with an exponential curve as in Figure 2A so that the humidity level required to induce a certain lamellar spacing (i.e. a certain percentage of dsDNA and bDDAB) can be calculated.

The shown data indicates that a structural transition occurs at 60% R.H. with structural stability at lower R.H. (indicated by the relatively consistent lamellar spacing) and significant structural dependence on R.H. values greater than 60%. We concluded that humidity levels of greater than 60% induce switching of the film structure from ssDNA/mDDAB to dsDNA/bDDAB and that the structural change continuously increases once the humidity is above the threshold level. We believe that the structure of the films at 60–75% R.H. is intermediate between the typical dry film (ssDNA/mDDAB) and wet film (dsDNA/bDDAB) structure and exists as a kind of two-phase system. These data support the FT-IR studies where the transition occurs only at high humidity levels, similar to the FT-IR analysis for the first minutes of the drying of the wetted DNA-DDAB film (Figure 1A and 1B). Based on our humidity measurements and on data from the literature we conclude that when the humidity drops below a certain threshold level the DNA double helix is no longer stable and the DNA is predominantly single-stranded with exposed bases that can mix with the hydrophobic DDAB tails.<sup>36</sup>

We also measured the change in q-value during drying of a water-immersed film by synchrotron SAXS experiments (Figure S9B), using a protocol similar to the FT-IR studies. While the film preparation was identical, the drying conditions were slightly different, resulting in a relatively slower structural transition (see Materials and Method). The main scattering peak of the dry film (ssDNA/mDDAB) was noted to be 2.15 nm<sup>-1</sup> and the main scattering peak of the wet film (dsDNA/bDDAB) was noted to be 1.45 nm<sup>-1</sup>, allowing allowing us to monitor the drying process in way that was similar to the FT-IR experiments. The k-value (slope) calculated from the exponential curve fitting (Figure 2B; 0.008± 0.001 seconds<sup>-1</sup>) is nearly identical to that measured by FT-IR, indicating that the two methods are sufficiently comparable and that the timing of the film's switching is unchanged, regardless of drying conditions or film thickness.

The structural changes induced by the relative humidity were reproducible in SAXS experiments where the films were cycled between dry and wet conditions and measured in each state. The obtained data shown in Figure 2C indicate that the film can continuously and reversibly switch its structure between ssDNA/mDDAB and dsDNA/bDDAB over several cycles, triggered by the water content of the surrounding environment. Interestingly the peak positions of all dry and wet films do not change between cycling, respectively. We initially expected that the films would become more ordered after several switching cycles, which should result in a sharper scattering peak with smaller peak half widths, indicating a larger domain size. However as there is no change in the peak widths we conclude that the domain size and structural order do not change during wet and dry cycling, possibly indicating that the DNA and DDAB molecules do not separate far from their partners in terms of physical distance when the switching occurs from a wet to dry film as described above as the molecular diffusion is likely very slow in this highly viscous solid film even when water is present. This leads to a partial explanation as to why the ssDNA strands can find their partner easily when the film is re-hydrated.

### Effect of Temperature on the DNA-DDAB films

In addition to the relative humidity temperature is expected to be a strong influence on the film's structure as it is the main physical influence that can reversibly denature DNA.<sup>37</sup> This denaturation process can be followed by various spectrophotometric techniques. We chose circular dichroism (CD) spectroscopy as a method to determine whether the DNA in the film was single or double stranded by measuring its helical content as reported previously.<sup>1</sup> The helical structure of B-form dsDNA can be identified by an negative peak at ~245 nm and positive peak at ~280 nm.<sup>38</sup> The DNA is likely single stranded in the dry DNA-DDAB film and therefore no such peaks should be seen as the dry film is heated. This was confirmed by temperature-resolved CD spectroscopy (Figure 3A) as well as temperature-controlled SAXS measurements (Figure 3B and 3C).

Within the CD spectra the dry DNA-DDAB film displayed a weak minimum peak at 245 nm independent of temperature in the range measured, indicating that the DNA in the film is likely single-stranded (Figure S11A). In contrast the water-immersed DNA-DDAB film (Figure S11B) showed a peak at 245 nm at room temperature ( $\sim 20^\circ\text{C}$ ) indicating that the complexed DNA in the wet film is helical and likely double stranded, in agreement with previous findings.<sup>1</sup> However when the temperature increased, the peak at  $\sim 245$  nm decreased which corresponds to the denaturation of dsDNA to ssDNA and the decreasing amount of helical structure, similar to native DNA in water (Figure S11C). At high temperatures between 85 and  $100^\circ\text{C}$  the spectra of both wet and dry films are unchanged, and so we conclude that the DNA is likely single-stranded in both films. The peak shifts observed (280 nm to 286 nm and from 240 to 245 nm) between the spectrum of native DNA to that of DDAB-complexed DNA derive from the hydrophobic environment of the DDAB molecules that surround the DNA in the complex, also known as the bathochromic effect or red shift (Figure S10).

The melting temperature ( $T_m$ ) of DNA was determined for the dry and wet films as well as native B-form DNA in water (Figure 3A), using a Boltzmann curve fit (see Materials and Method). The peak intensity of the native DNA at 240 nm was higher compared to that of the DNA-DDAB film, indicating that native DNA has greater helical character than the DNA in the film. The apparent melting temperature of DNA in the water immersed DNA-DDAB film was determined by this method to be  $\sim 63^\circ\text{C}$  compared to  $\sim 71^\circ\text{C}$  for native DNA. Native DNA has a defined melting point and narrow melting range of a range of  $2.7^\circ\text{C}$  as seen by a sharp change in CD signal. The increase in CD signal or melting curve of the complexed DNA in the film was much broader and occurred over a larger range of  $12^\circ\text{C}$ . We assume that the DNA molecules are entangled (as is common with long polymers) and intertwine between several lamellar layers in the DNA-DDAB film which could explain the wider range of melting as the film is less ordered or “pure”. In addition the hydrophobic presence of DDAB decreases the melting point of the DNA as discussed in the literature for DNA measured in organic solvents.<sup>21,22,24,25</sup> No melting temperature could be measured for the DNA in the dry film as it is single-stranded and cannot denature.

To confirm the melting processes SAXS studies were performed showing that the  $q$ -value of the wet film at room temperature increased from  $1.45\text{ nm}^{-1}$  (4.4 nm lamellar spacing) to  $1.75\text{ nm}^{-1}$  (3.6 nm lamellar spacing) as the film was heated from 25 to  $90^\circ\text{C}$  (Figure 3B). As seen for the CD measurements this transition happens continuously as opposed to instantly. At room temperature the main scattering peak at  $1.45\text{ nm}^{-1}$  (4.4 nm lamellar spacing) is present. As the temperature rises to  $40^\circ\text{C}$  the peak broadens and at  $60^\circ\text{C}$  a second peak at  $1.75\text{ nm}^{-1}$  (3.6 nm lamellar spacing) can be observed. This second peak increases in intensity as the film is heated further to  $70^\circ\text{C}$  and becomes the dominant peak when the film is heated above  $80^\circ\text{C}$ . Since there are two peaks within the broad peak at high temperature ( $1.45\text{ nm}^{-1}$  and  $1.75\text{ nm}^{-1}$ ), presumably composed of ssDNA and dsDNA, we have additional evidence that the DNA does not fully separate when heated to and above its apparent melting temperature according to the CD data (which does not measure the true melting temperature but changes in helicity). Since we have reasonable evidence that the DNA becomes single stranded during heating (as its lamellar spacing decreases from 2.0 nm at room temperature to 1.1 nm at  $85^\circ\text{C}$ ), DDAB must then remain in a bilayer (2.4 nm) in the heated film to account for the measured spacing. We can therefore assume that the structure of DDAB in the film does not depend on the DNA secondary structure because the bDDAB structure is not affected by the DNA melting or by high temperature in water, but essentially only depends on the water content. This result reflects the assumption of earlier studies where it was mentioned that DNA-lipid complexes used in gene delivery tend to assume the structure preferred by the lipid used<sup>9,10</sup>.

Interestingly the ratio of the integrated peak intensities at  $1.45\text{ nm}^{-1}$  and  $1.75\text{ nm}^{-1}$  reflect the melting process of the DNA measured by CD spectroscopy nearly completely. The melting

transition of the DNA in the complex film occurred slowly over a wide range of temperature and was lower compared to native DNA, as previously seen in Figure 3A. We also could demonstrate that the DNA-DDAB film is structurally undamaged by heat even after several heating and cooling cycles (Figure 3C) since the peak positions within the SAXS spectra are not changed between respective cycles.

The dry films however showed nearly no influence on the lamellar spacing. Only an increase in the  $q$ -value from  $2.15 \text{ nm}^{-1}$  (2.93 nm lamellar spacing) to  $2.25 \text{ nm}^{-1}$  (2.8 nm lamellar spacing) was observed. We assume that the temperature increases the mobility of the molecules, especially of the aliphatic chains of the DDAB, and allows for a higher packing density compared to the film at lower temperature (Figure S12).

The various structural states of the surfactant and the nucleic acid within the film described so far are summarized as illustrations in Figure 4: bDDAB paired with dsDNA stabilized by hydrogen bonds between the bases in the wet film, bDDAB paired with ssDNA in the heated wet film, and mDDAB paired with dsDNA in the dry film. While the structure of the DNA at high temperature in water is known, the influence of the DNA structure on the assembly of the DDAB molecules is unclear. The DDAB molecules can remain as mDDAB between ssDNA, similar to the dry state, or as a bDDAB, similar to the wet state, indicating that the film structure has greater flexibility than was previously supposed.

### Stabilization of the DDAB bilayer by cholesterol

Since bDDAB remains stable in the wet film even when the DNA melts due to high temperature<sup>39</sup>, we were therefore interested to create modified films that retain bDDAB even in the dry state. It is known in the literature that cholesterol has the ability to stabilize lipid bilayers by penetrating into the hydrophobic aliphatic chains,<sup>40</sup> which allows cell walls to stay fluid at body temperature. It is also known that the bilayer thicknesses of unsaturated phospholipids with an alkyl chain length of 12–16 carbons increase linearly with the amount of added cholesterol, mostly by overcoming the tilt of the bilayer tails. However with longer tail length and lower temperatures the lipid bilayer decreases in width (unless the lipid becomes unsaturated).<sup>41,42</sup> As DDAB is a surfactant with two 12-carbon tails we expected to see the same effects of cholesterol intercalation into the bilayer with an increase in lamellar spacing as described above for phospholipids. As a side effect of this intercalation we hoped to stabilize the bDDAB against environmental factors. To date many studies have been published on cholesterol-modified DNA-surfactant complexes, which include various cationic surfactants including DDAB.<sup>43,44</sup> However to date only a few publications deal with the effect of cholesterol on dry DNA-lipid or DNA-surfactant films. To investigate the role of cholesterol in the dry film, different amounts of cholesterol were mixed with the DNA-DDAB complexes, dissolved in isopropanol, and then cast as a film on a solid substrate (see Materials and Method). Based on data from the literature, addition of cholesterol would be expected to stabilize the bilayer (DDAB) as shown in the expected structures of the cholesterol films in the wet and dry states in Figure 5A.

The SAXS spectra of the cast dry cholesterol films (Figure 5B) indicated that indeed bDDAB remains stable in the presence of cholesterol as evidenced by the decreasing  $q$ -value from  $2.2 \text{ nm}^{-1}$  to  $1.8 \text{ nm}^{-1}$ , corresponding to an increase in the lamellar spacing from 2.8 nm to 3.5 nm with increasing amounts of added cholesterol. We observed the switching transition of the dry films between 10% and 20% of added cholesterol. At lower cholesterol content the peak stayed at  $2.2 \text{ nm}^{-1}$  while at higher cholesterol content it shifted to  $1.8 \text{ nm}^{-1}$ . Since this shift does not happen continuously with increasing amounts of cholesterol, we assume that a structural change takes place. We presume that either the added cholesterol decreases the amount of interdigitation in bDDAB, accounting for the increased spacing or that the cholesterol tends to stabilize the bilayer of DDAB molecules even in the dry state. Based on the fact that the shift

happens stepwise we assume that DDAB forms a bilayer at higher cholesterol content while at lower cholesterol content the DDAB remains in a monolayer.

In contrast, the SAXS spectrum of the wet cholesterol films (Figure 5C) show that the lamellar spacing for these films is much larger due to the presence of dsDNA and increases with increasing amounts of cholesterol, again presumably due to decreased interdigitation in bDDAB. The stability of the DDAB bilayer with added cholesterol is indicated in Figure S13, as the FT-IR DDAB peak ratio remains very constant. Interestingly dsDNA seems to be stabilized by larger amounts of cholesterol (as indicated by the increasing FT-IR peak ratio), which we attribute to the fact that cholesterol tends to retain more water in the film due to its hydrophilic headgroup. When the wetting and drying FT-IR measurements were performed on a 20% cholesterol film, the  $k$  values calculated for the peak ratio variations of DNA and DDAB (Figure 5D) were approximately triple that of the  $k$  values for normal films (0.033 for cholesterol films versus 0.017 or 0.011 for normal films), from which we conclude that addition of cholesterol to the films increases their speed of switching ability. This may be because the decrease in interdigitation of DDAB allows the tails to untangle and separate more easily. The starting point of data analysis within the graph was placed at the point when the maximum peak ratio of the DNA was reached and then started to decrease. Interestingly the DDAB peak ratio started to decrease approximately 100 seconds before the DNA peak ratio until eventually a certain peak ratio threshold was reached for both components. On reaching this threshold the DNA began to become single stranded. This may indicate that bDDAB initiated the switching, although this is not clear. In summary the FT-IR data indicated that bDDAB is not stabilized by the addition of cholesterol to the DNA-DDAB films; however the cholesterol appears to decouple the switching transitions of DNA and DDAB.

#### Effect on the DNA-DDAB film structure by nucleic acid intercalation of ethidium bromide

Ethidium bromide was previously used as a fluorescent marker to observe the state of the DNA in the cast film<sup>1</sup> as it is able to intercalate into dsDNA and serves as a fluorescent marker for it.<sup>45</sup> However the total amount of ethidium bromide intercalated in the film after casting was unknown to date. The anticipated structures of the ethidium bromide-labeled film in the wet and dry states are shown in Figure 6A, with ethidium bromide (in green) intercalated between the DNA base pairs in the wet state and associated with the exposed hydrophobic DNA bases in the dry state, possibly through base stacking interactions. Intercalation experiments were done wherein dsDNA molecules were labeled with varying amounts of ethidium bromide (Figure 6B, top) followed by complexation with DDAB (Figure 6B, bottom, Figure S14). It was found that the correlation between the amount of DNA base-pairs labeled with ethidium bromide in native DNA (i.e. before complexation with DDAB) and the amount labeled in the DNA-DDAB complex (i.e. DNA after complexation) is nearly linear in the region measured (Figure S15). We also measured the fluorescence over time of a wetted ethidium bromide film as it dried (Figure 6C) and as reported in a previous publication<sup>1</sup>, the fluorescence was high in the wet film and decreased during drying, indicating a structural change in DNA from double-stranded in the wet film to single-stranded in the dry film as the water evaporated.

We next measured the switching times of DNA and DDAB in a film that had been labeled with ethidium bromide at every 10<sup>th</sup> base pair and immersed in water for 5 minutes before drying by monitoring fluorescence intensity (Figure S16) and summarizing the FT-IR peak ratios in the DNA and DDAB regions over time (Figure 6D). Although it was expected that the presence of ethidium bromide would stabilize dsDNA by reinforcing the base-stacking interactions and delay its switching relative to DDAB, we instead found that the DNA was able to switch before the DDAB, as indicated by a comparatively early decrease in its peak ratio relative to DDAB, although their  $k$  values were identical. Possibly as the film dries and its environment becomes more hydrophobic the ethidium bromide may prefer to associate with the hydrophobic DDAB



tails rather than the DNA bases, as we see no phase separation of the ethidium bromide upon drying. The loss of ethidium bromide with increasing hydrophobicity may encourage the DNA to unzip and reveal its hydrophobic bases. The switching of DDAB may also be somewhat delayed as it must accommodate ethidium bromide as it switches from a bilayer to a monolayer.

The films were measured both wet (Figure 6E) and dry (Figure 6F) using SAXS. The  $q$ -value of the sharp DNA peak was consistent within each set of conditions and did not vary significantly with the amount of ethidium bromide intercalated, as ethidium bromide has little effect on ssDNA and cannot intercalate to increase the thickness of the strands. We did observe a small decrease in the  $q$ -value of the main scattering peak in the dry film from  $2.15 \text{ nm}^{-1}$  to  $1.9 \text{ nm}^{-1}$  with the highest amount of ethidium bromide measured. One explanation for this increase in the lamellar spacing from 2.9 nm to 3.3 nm could be that ethidium bromide, being hydrophobic, would associate with the DDAB tails as well as the exposed hydrophobic DNA bases. This slight disruption in structure would explain the increase in the lamellar spacing. Within the water-immersed films a small decrease in the  $q$ -value from  $1.44 \text{ nm}^{-1}$  to  $1.37 \text{ nm}^{-1}$  was observed as the amount of ethidium bromide in the film increased. This increase of 0.2 nm in the lamellar spacing is presumably due to the increase in width of the DNA double helix (caused by the slight B- to A-form transition) when intercalated with ethidium bromide.<sup>46</sup> Another possibility would be that a portion of ethidium bromide is trapped in mDDAB after having been expelled from the denaturing DNA which would also increase the lamellar spacing.

### Macroscopic behavior and simulated film disassembly

We have seen that the structure of DNA in the cast film can be reversibly altered by physical influences like temperature and humidity while the components can be altered with a chemical additive like cholesterol or ethidium bromide. However, we have only demonstrated these effects on the molecular, as opposed to macroscopic, scale. We have studied the swelling behavior of a thick DNA-DDAB film which was cast in a mold with the dimensions of 17 mm  $\times$  17 mm  $\times$  20 mm (see Materials and Method). When this film was removed from the mold and immersed in water, the size and weight of the film increased till a plateau was reached after 150 seconds, the opposite of the drying procedure and in approximately the same amount of time (Figure 7A). Interestingly the volume of the thick film increased by 157% (from initial dimensions of 17 mm  $\times$  17 mm  $\times$  0.9 mm to final dimensions of 19 mm  $\times$  19 mm  $\times$  1.2 mm), which is the same percentage as the increase in the lamellar spacing from the dry to the wet film (2.8 to 4.4 nm), and was confirmed by several repeated cycles. The hydration rate was determined with an exponential fit to be  $y = 1.562 - 0.5528 e^{(-0.2147 \cdot \text{time})}$  which is comparable to the drying (dehydration) rate. Therefore there is a connection between the nanoscopic structural transition and macroscopic swelling of the film, as noted previously.<sup>1</sup> The film dimensions also increased by the same ratio in each direction, indicating that the swelling was uniform. The density of a similar thick film (33 mm  $\times$  14.5 mm  $\times$  2 mm with a weight of 948 mg) was measured to be  $0.99 \text{ g/cm}^3 \pm 10\%$ , similar to a hydrogel.

One possible application of these films is to use them as drug delivery vehicles. Intercalating drugs such as daunorubicin can be blended with dsDNA and released as the films disassemble *in vivo* (as dsDNA is presumably degraded by nucleases); although until now it was not clear by which mechanism the films would degrade. We simulated disassembly *in vivo* by adding 10  $\mu\text{L}$  of 1X PBS buffer in one spot on top of an ethidium bromide-labeled film (Figure S17) and as the film dried it appeared to dissolve or break apart. In the center of the spot where PBS had been added was a translucent aggregate while the area surrounding it was smooth (Figure 7B). The aggregate was fluorescent while the smooth area surrounding it was dark (Figure 7C), which led us to conclude that as the film dissolved the ethidium bromide-labeled dsDNA had hybridized and aggregated in the center, presumably due to its greater viscosity and size, and the DDAB had separated to the outside. Ions could screen the charges of both DNA and DDAB,



reducing their ability to electrostatically bind, and therefore the addition of the buffer led to dissolution of the film in the spot where it had been added. At the edges of this spot the film showed evidence of a lamellar structure through exposed step formations (Figure 7D). These steps were observed to fluoresce at their edges (Figure 7C and D), indicating that exposed dsDNA was present. We assume that the DNA was allowed to hybridize as the surrounding DDAB layers were dissolved away by PBS. By using optical microscopy coupled with atomic force microscopy (AFM) we were able to demonstrate that the step height of one layer to the next is 2.8 nm (Figure 7E), the same as the dry film's lamellar spacing and the step height measured by AFM in an earlier work.<sup>1</sup> We can therefore conclude that the disassembly of the film occurs layer by layer.

## Conclusion

We have discussed the structural behavior of DNA-DDAB films in detail and investigated the structural changes occurring in the nucleic acid and surfactant in response to the surrounding environment such as the water content, relative humidity level, temperature, as well as the effect of additives that tend to intercalate either into either DDAB or DNA. The switching of DNA and DDAB occurs virtually simultaneously and the rate constant ( $k$ ) of their transition from dsDNA to ssDNA and bDDAB to mDDAB in a drying film as measured by FT-IR are nearly identical. However, it is therefore difficult to know whether DNA or DDAB, if either, is responsible for initiating the switching from these data. We conclude that the structure of DNA in the film depends on the hydrophobicity and temperature of the environment, while the state of DDAB depends essentially only on the hydrophobicity. The structure of the film is quite flexible, and can be altered by changing environmental conditions as well as by chemical additives. Structural change with varying humidity levels is generally continuous, although after reaching a threshold value of 60 % R.H. the transition from ssDNA and mDDAB to dsDNA and bDDAB occurs more rapidly.

High temperatures above 70 °C only have an effect on the structure of DNA within the wet film, since although the DNA remains double stranded at low temperatures, it increasingly becomes single stranded due to the melting of the hydrogen bonds that hold the two strands together when the temperature is raised. The measured melting temperature of DNA complexed in the film is slightly lower and spans a wider temperature range than that of native DNA, presumably due to the presence of DDAB. The DDAB bilayer structure is not affected however by the melting of DNA and remains in a bilayer regardless of increased temperature in the range measured. No temperature-related structural effects were seen for the dry film as heat can have no structural effect on ssDNA and mDDAB. We assume, based on the stable behavior of bDDAB in the wet state and the possibility to generate ssDNA with bDDAB that DDAB dictates the switching behavior of the film, although this is not evident from the FT-IR data. The films also seem to be thermostable as the lamellar spacing of DNA-DDAB unit values of the main scattering peaks of the wet and dry film do not change, respectively, after several cycles.

Cholesterol was used to influence the switching behavior of the films and delay the switching transition of DNA relative to DDAB when a wet film was dried, presumably due to retention of water by cholesterol in the film which stabilized dsDNA. When a certain threshold amount of DDAB switched from a bilayer to a monolayer the transition of DNA was triggered from a double to single-stranded state, indicated by the delayed switching of DNA relative to DDAB. Interestingly despite our expectation that cholesterol would stabilize bDDAB we could not find any evidence for it. The DNA-intercalating agent ethidium bromide was used to study the effect of a DNA chemical additive in contrast to cholesterol, a chemical additive for DDAB. Ethidium bromide intercalates only in dsDNA and therefore only in a wet film and not for ssDNA in a dry film. We assume that ethidium bromide, being hydrophobic, associates with

the DDAB tails as well as the exposed bases of ssDNA in the dry film, and contributes to the delayed switching of DNA in a drying film relative to DDAB.

Finally, we investigated the degradation potential of the films in buffer. The volumetric swelling of the film on a nanoscopic level is related to the macroscopic swelling of a thick film. Also the film was observed to disassemble layer-by-layer when exposed to buffer (such as PBS) due to electrostatic screening of the charges by salts, which makes it reasonable to suppose that the film will disassemble easily *in vivo* and can act as a drug delivery vehicle. A recent report of solid DNA-cationic polymer films embedded with functional aptamers is evidence of a possible application for films such as ours.<sup>47</sup>

In conclusion, we have found that the structure of DNA-DDAB is quite flexible in response to various physical conditions (heat and humidity) as well as chemical ones (addition of cholesterol and ethidium bromide).

## Supplementary Material

Refer to Web version on PubMed Central for supplementary material.

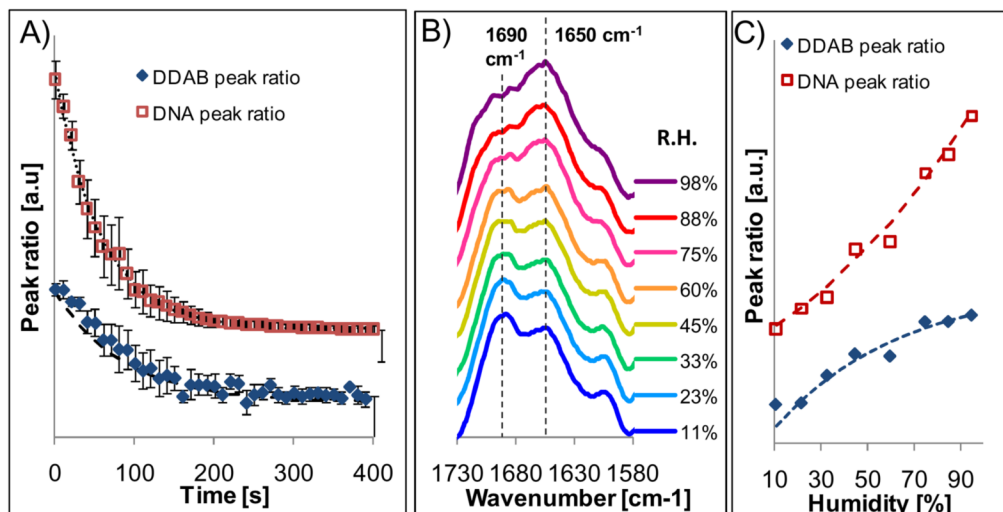
## Acknowledgments

The authors would like to acknowledge support under the MRSEC Program of the National Science Foundation under Award of DMR05-20415 (L.J. + M.T.), DMR-0710521 (Materials World Network) (M.T.) and the National Institutes of Health under grant R01 GM079604-01(L.J.). L.J. would like to dedicate this article to Professor Jérôme Lejeune.

## References

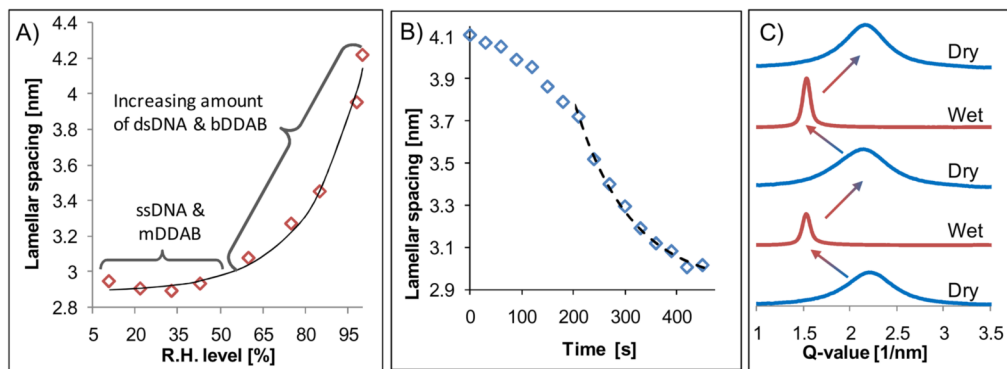
1. Neumann T, Gajria S, Tirrell M, Jaeger L. *J Am Chem Soc* 2009;131:3440–3441. [PubMed: 19275252]
2. Ijiro K, Okahata Y. *J Chem Soc-Chem Commun* 1992:1339–1341.
3. Hoshino Y, Tajima S, Nakayama H, Okahata Y. *Macromol Rapid Commun* 2002;23:253–255.
4. Radler JO, Koltover I, Salditt T, Safinya CR. *Science* 1997;275:810–814. [PubMed: 9012343]
5. Martin B, Aissaoui A, Sainlos M, Oudrhiri N, Hauchecorne M, Vigneron JP, Lehn JM, Lehn P. *Gene Ther Mol Biol* 2003;7:273–289.
6. Templeton NS, Lasic DD, Frederik PM, Strey HH, Roberts DD, Pavlakis GN. *Nature Biotech* 1997;15:647–652.
7. Caracciolo G, Sciubba F, Caminiti R. *App Phys Lett* 2009;94:153901-1–153901-3.
8. Felgner PL, Gadek TR, Holm M, Roman R, Chan HW, Wenz M, Northrop JP, Ringold GM, Danielsen M. *Proc Nat Acad Sci USA* 1987;84:7413–7417. [PubMed: 2823261]
9. Boussein NF, McAllister CS, Ewert KK, Samuel CE, Safinya CR. *Biochemistry* 2007;46:4785–4792. [PubMed: 17391006]
10. Gawrisch K, Parsegian VA, Hajduk DA, Tate MW, Gruner SM, Fuller NL, Rand RP. *Biochemistry* 1992;31:2856–2864. [PubMed: 1550812]
11. Smitthipong W, Neumann T, Gajria S, Li Y, Chworos A, Jaeger L, Tirrell M. *Biomacromolecules* 2009;10:221–228. [PubMed: 19099365]
12. Dubois M, Zemb T. *Langmuir* 1991;7:1352–1360.
13. Almgren M, Edwards K, Karlsson G. *Colloids Surf, A* 2000;174:3–21.
14. Naji A, Jungblut S, Moreira AG, Netz RR. *Physica A* 2005;352:131–170.
15. Young JF. *J Appl Chem* 1967;17:241–245.
16. Winston PW, Bates DH. *Ecology* 1960;41:232–237.
17. O'Brien FEM. *J Sci Instrum* 1948;25:73–76.
18. Hull MC, Cambrea LR, Hovis JS. *Anal Chem* 2005;77:6096–6099. [PubMed: 16159147]
19. Leal C, Sandström D, Nevsten P, Topgaard D. *Biochim Biophys Acta* 2008;1778:214–228. [PubMed: 18320639]

20. Harries D, Podgornik R, Parsegian VA, Mar-Or E, Andelman D. *J Chem Phys* 2006;124:224702-1–224702-14. [PubMed: 16784296]
21. Baldini G, Huang FH, Varani G, Cordone L, Fornili SL, Onori G. *Il Nuovo Cimento D* 1985;6:618–630.
22. Lee CH, Mizusawa H, Kakefuda T. *Proc Nat Acad Sci USA* 1981;78:2838–2842. [PubMed: 7019913]
23. Panjkovich A, Melo F. *Bioinformatics* 2005;21:711–722. [PubMed: 15501913]
24. Herskovits T, Singer SJ. *Archiv Biochem Biophys* 1961;94:99–114.
25. Sinanoglu O, Abdunur S. *Photochemistry and Photobiology* 1964;3:333–342.
26. Levine L, Jencks WP, Gordon JA. *Biochemistry* 1963;2:168–175. [PubMed: 13930149]
27. Zemb T, Belloni L, Dubois M, Marcelja S. *Prog Colloid Polym Sci* 1992;89:33–38.
28. Zemb T, Gazeau D, Dubois M, Gulik-Krzywicki T. *Europhysics Letters* 1993;21:759–759.
29. Chen FY, Hung WC. *Chinese Journal of Physics* 1996;34:1363–1372.
30. Dubois M, Zemb T, Fuller N, Rand RP, Parsegian VA. *J Chem Phys* 1998;108:7855–7869.
31. Feitosa E, Alves FR, Niemiec A, Real OME, Castanheira EM, Baptista AL. *Langmuir* 2006;22:3579–3585. [PubMed: 16584229]
32. Lvov, Y.; Möhwald, H. *Protein Architecture: Interfacing molecular assemblies and immobilization biotechnology*. CRC Press; 2000.
33. Zhou J, Gregurick SK, Krueger S, Schwarz FP. *Biophysical Journal* 2006;90:544–551. [PubMed: 16258042]
34. Saenger W. *Ann Rev Biophys Chem* 1987;16:93–114.
35. Podgornik R, Rau DC, Parsegian VA. *Macromolecules* 1989;22:1780–1786.
36. Pilet J, Brahm J. *Biopolymers* 1973;12:387–403.
37. Cavalieri LF, Small T, Sarkar N. *Biophysical Journal* 1962;2:339–350. [PubMed: 13877444]
38. Johnson, W. *Spectroscopic and Kinetic Data. Physical Data I. Vol. 1C*. Springer-Verlag; 1990.
39. Caboi F, Monduzzi M. *Langmuir* 1996;12:3548–3556.
40. Garcia RA, Pantazatos SP, Pantazatos DP, MacDonald RC. *Biochimica Et Biophysica Acta-Biomembranes* 2001;1511:264–270.
41. McIntosh TJ. *Biophysical Journal* 1978;21:A123–A123.
42. Kucerka N, Pencer J, Nieh MP, Katsaras J. *European Physical Journal E* 2007;23:247–254.
43. Callow P, Fragneto G, Cubitt R, Barlow DJ, Lawrence MJ. *Langmuir* 2008;25:4181–4189. [PubMed: 19714835]
44. Marty R, N'Soukpoe-Kossi CN, Charbonneau D, Weinert CM, Kreplak L, Tajmir-Riahi HA. *Nucleic Acids Research* 2009;37:849–857. [PubMed: 19103664]
45. Houssier C, Hardy B, Fredericq E. *Biopolymers* 1974;13:1141–1160. [PubMed: 4859366]
46. Nafisi S, Saboury AA, Keramat N, Neault JF, Tajmir-Riahi HA. *J Mol Struc* 2007;827:35–43.
47. Sultan Y, Walsh R, Monreal C, DeRosa MC. *Biomacromolecules* 2009;10:1232–1237.



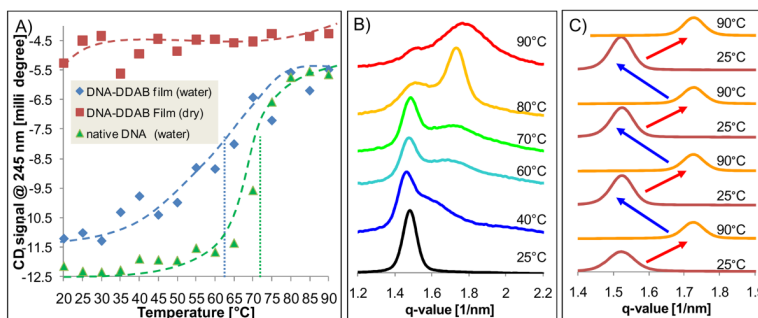
**Figure 1.**

(A) Summary of FT-IR spectra of the DNA base pair region taken every ten seconds as a water-immersed film dried for 400 seconds. Decrease in the peak ratios of 1690 to 1650  $\text{cm}^{-1}$  of the DNA base pair and DDAB tail regions averaged over four sequential measurements with error bars showing the standard deviation for each point. The DDAB values are amplified by a factor of 60 compared to the DNA values for comparison purposes. The peak ratio decreases (and therefore the structural switching of DNA and DDAB) occur virtually simultaneously, as indicated in the k values of the exponential curve fit. The curve fit for the DNA peak ratio is  $y = 1.577 + 2.563 \cdot e^{(-0.017 \cdot \text{time})}$  and the curve fit for the DDAB peak ratio is  $y = 0.846 + 1.098 \cdot e^{(-0.011 \cdot \text{time})}$ . (C) FT-IR spectra of the DNA base pair region of a cast film at different relative humidity (R.H.) levels showing the gradual transition from ssDNA (11% R.H.) to dsDNA (95% R.H.). Dotted lines indicate the peak positions at 1650 and 1690  $\text{cm}^{-1}$ . (D) Peak ratio intensities of the DNA base pair and DDAB tail regions increase with increasing humidity levels, again showing the nearly simultaneous structural transition of DNA and DDAB.



**Figure 2.**

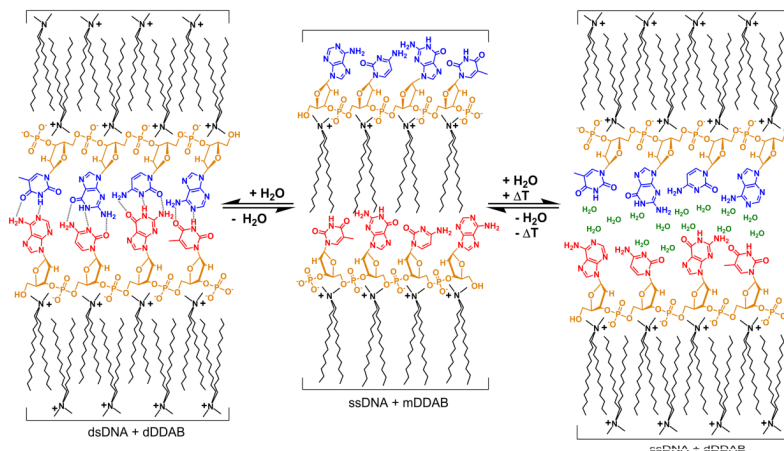
Small angle X-ray (SAXS) scattering of the DNA-DDAB films at various humidity levels. An increase in humidity leads to a structural swelling of the film with a correspondingly increasing lamellar spacing (A). The black dotted line indicates the shift of the main scattering peak with increasing humidity. The transition begins to occur more dramatically at a threshold value of approximately 60% R.H. which agrees with FT-IR measurements. The exponential curve fit is  $y = 0.01 \cdot e^{0.05x} + 2.90$ . The timing of this transition was monitored by synchrotron SAXS experiments using a water-immersed cast film. The black line indicates the position of the main scattering peak at various humidity levels (B). The slope of the decrease in lamellar spacing as the film dries is nearly identical to the slope of the decrease in peak ratios measured by FT-IR, indicating that the two techniques are sufficiently comparable and that the timing of the film's switching is unchanged regardless of drying conditions and film thickness. The structural transition caused by hydration and dehydration is fully reversible (C) which could be seen in the identical peak width and q-value for all wet and dry films, respectively.



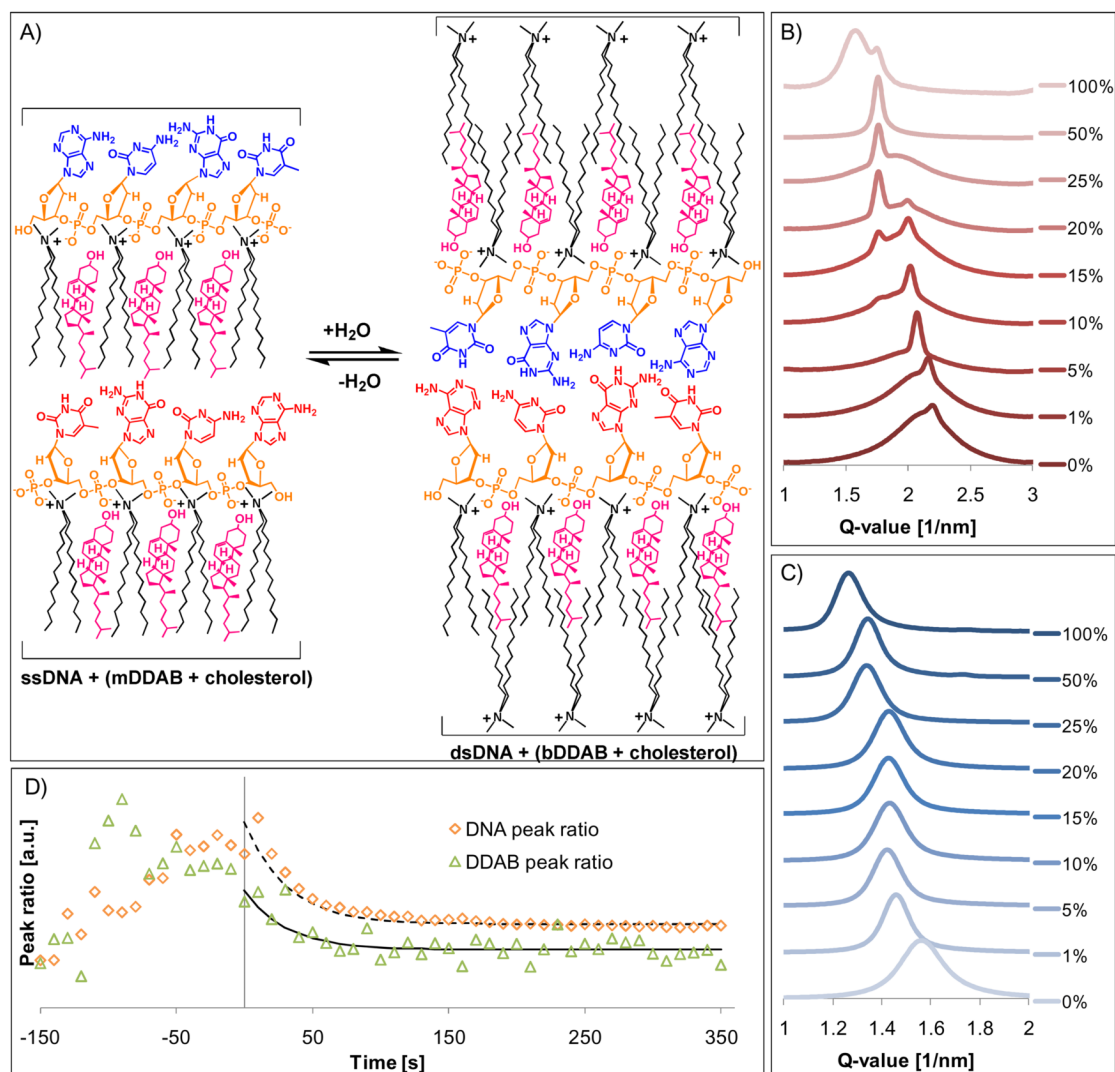
**Figure 3.**

Temperature response of the DNA-DDAB films. By comparing the peak value at 245 nm in the CD-spectra of native DNA and a wet and dry film during the same heating process and using a Boltzmann curve fitting (A), the melting temperature of DNA in the wet film is ~63.1 °C, compared to ~71.2 °C for native DNA, a decrease presumably due to complexation of DNA by DDAB which reduces backbone repulsion between the two strands which would lower the melting point. The T values for each curve indicate the broadness (i.e. the homogeneity of helical DNA), as measured in degrees Celsius, of the DNA melting point. No reasonable melting temperature could be obtained for the DNA in the dry film, indicating that it is single-stranded and cannot melt. Similar behavior was noted in the SAXS spectra of wet (B) and dry DNA films (Supporting Information Figure S11). As the temperature increases the q-value of the main scattering peak of the wet DNA-DDAB film increases and the lamellar spacing correspondingly decreases from 4.4 to 3.6 nm, suggesting that the heated wet film consists of bDDAB (2.4 nm) + ssDNA (1.1 nm). The CD results in combination with SAXS (B) experiments of the wet film indicate that the DDAB remains in bilayer formation while the DNA becomes single stranded. The heat treatment, even after several cycles, does not change the structure of the wet film, indicating that it is thermostable (C).



**Figure 4.**

Expected states of DNA and DDAB in the cast film which can be reversibly altered by the surrounding conditions as summarized from the data in the above figures. The dry film consists of ssDNA and mDDAB (left) which changes to bDDAB paired with dsDNA when the film is immersed in water (middle). The DNA becomes single stranded in the presence of bDDAB when the temperature of the wet film is raised above the melting point of the nucleic acid (right) which is  $\sim 71^\circ\text{C}$  according to CD measurements (Figure 3A), and then anneals as the temperature is lowered. The water molecules fill the spaces between the separated DNA bases, though it is unknown how far the strands separate when heated.

**Figure 5.**

Cholesterol-blended DNA-DDAB films. (A) Expected structural change of the cholesterol-doped films between the dry and wet states. Cholesterol is shown in pink, inserted between the DDAB aliphatic tails though both DNA and DDAB are able to switch. (B) SAXS spectra of dry films with varying amounts of cholesterol. (C) SAXS spectra of the same films in the wet state. Both sets of data indicate that the lamellar spacing of the films increases with increasing amounts of cholesterol. Peak ratios in the DNA base-pair and DDAB tail regions of dry cholesterol films (see Figure S11 in the Supporting Information) indicate that DDAB remains largely in a bilayer while DNA becomes more double-stranded with increasing amounts of cholesterol, presumably due to the increased retention of water by cholesterol in the film. (D) Variations in the DNA and DDAB peak ratios in their respective regions over time in a wetted 20% cholesterol film as it dried. K values for the process are approximately triple that of normal DNA-DDAB films. The grey line indicates time of addition of water.

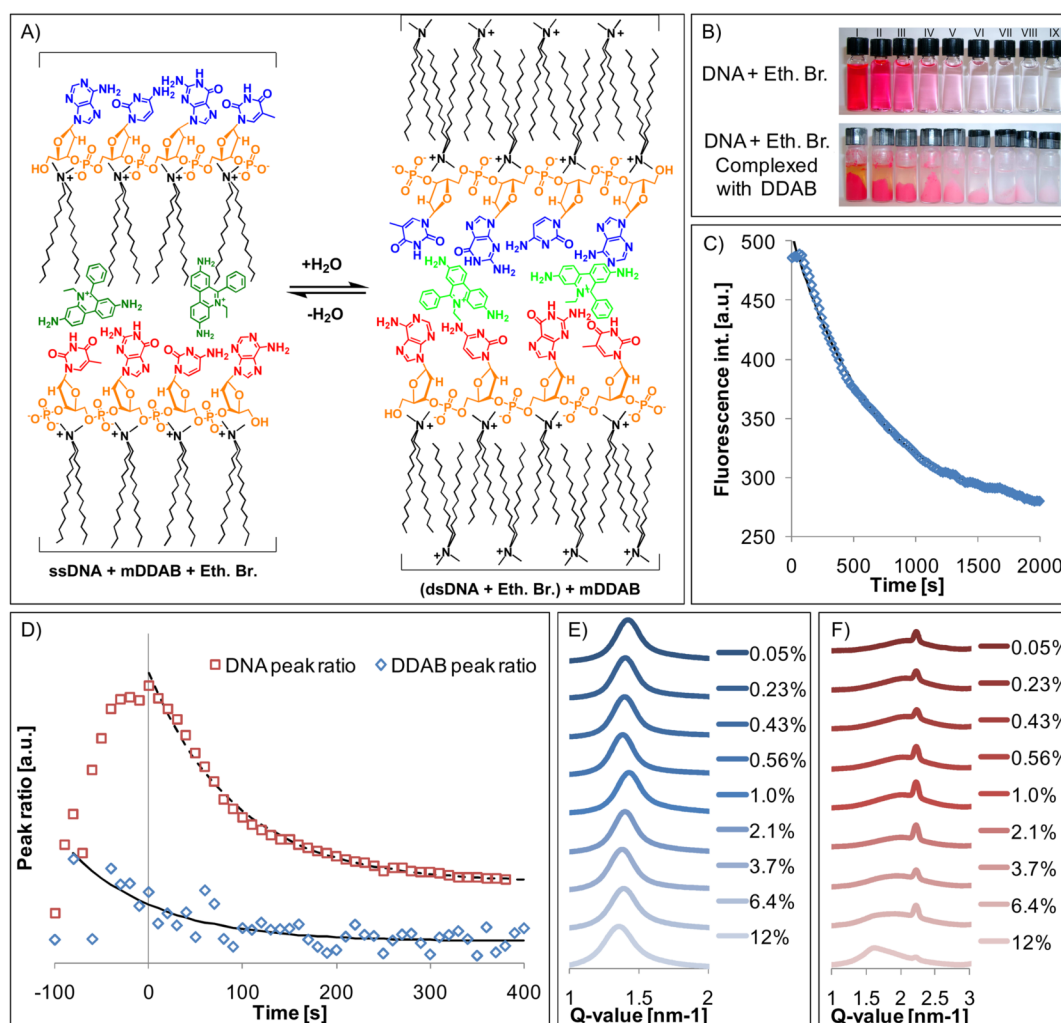


**Figure 6.**

Structural analysis of ethidium bromide-labeled films. (A) Expected structural change of the DNA-DDAB film with added ethidium bromide between the dry and wet states. Ethidium bromide is shown in green, intercalating between the DNA base-pairs in the wet state, while it associates both with the exposed hydrophobic DNA bases and DDAB tails in the dry state. (B) Photographs of aqueous solutions or suspensions of (top) DNA with varying amounts of ethidium bromide and (bottom) DNA-DDAB complexes labeled with ethidium bromide. The supernatant used in the UV-Vis studies to measure the amount of ethidium bromide intercalation is the liquid taken from the bottom row of suspensions (see Supporting Information, Figure S13). The numbers I-IX refer to varying percentages 0.05–12% ethidium bromide, respectively. (C) Decay in fluorescence over time of a wetted 6.4% ethidium bromide-labeled film as it dried, agreeing with earlier data that suggests DNA is double-stranded in the wet film and becomes single-stranded in the dry film, and thus can no longer intercalate ethidium bromide which can then no longer fluoresce. Curve fitting indicates that the decay is exponential. (D) Variations in the peak ratio of a 6.4% ethidium bromide wetted film as it dries over time fitted with an exponential curve equation. K values for both DNA and DDAB ratio decay are nearly identical to that of the normal DNA-DDAB films (see Figure 1). (E) SAXS spectra of wet films labeled with varying amounts of ethidium bromide. (F) SAXS spectra of the same films in the dry state.

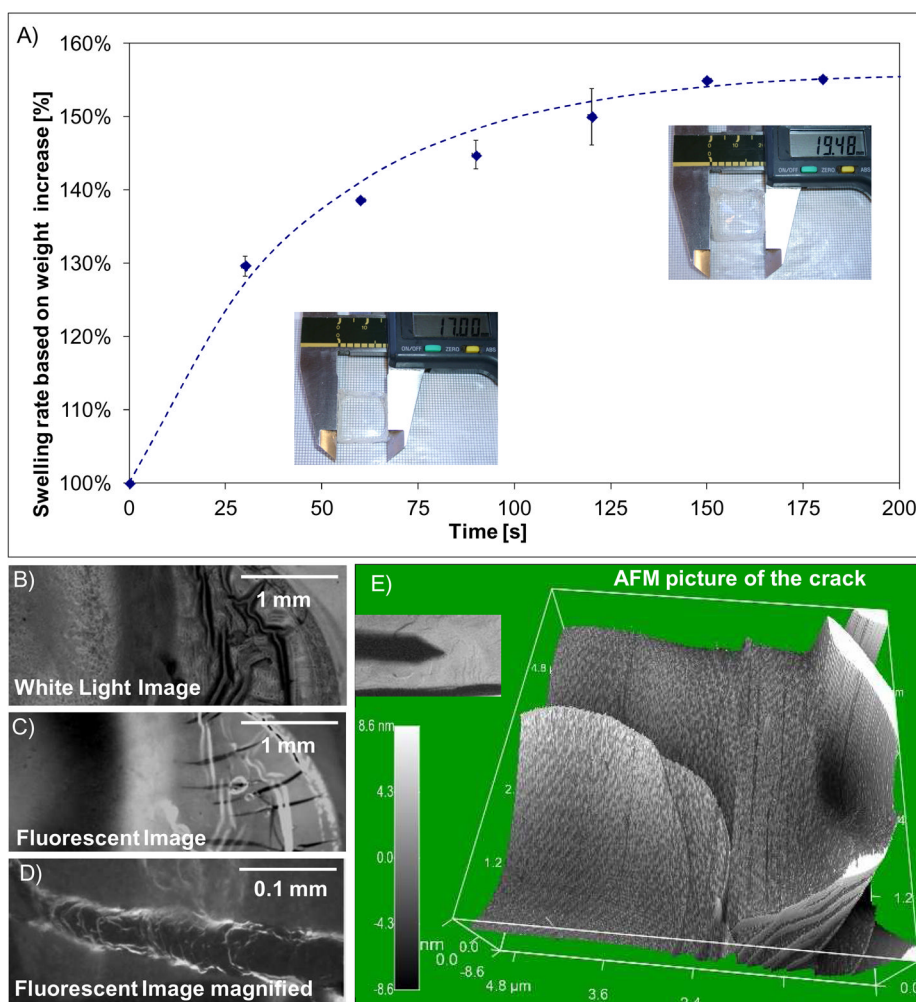


**Figure 7.**

Macroscopic swelling and degradation experiments of a cast film. The molecular transition between dry and wet films can also be observed in a thick film when the dry film is immersed in water, based on weight and size increase. (A) An increase of 155% in volume corresponds to the transition from the structure in dry state to the structure in wet state, which is the same percent increase in the lamellar spacing from the dry to wet film (2.8 to 4.4 nm), indicating a direct correlation between the macroscopic and nanoscopic film structure. The rate was determined with an exponential fit to  $y = 1.562 - 0.5528 e^{(-0.2147 \cdot \text{time})}$  which is comparable to the drying rate. (B-D) Fluorescent and white light images of an ethidium bromide-labeled film on top of which was added PBS buffer, causing the film to degrade. (B) White light microscope image of the area in which the buffer was added. (C) Fluorescent microscope image of the same region, showing the DNA aggregation (bright areas) separated from the DDAB (dark areas). (D) Close-up of the cracks at the edge of the PBS region, indicating step formation. (E) Analysis of the cracks in the film by AFM indicates that the film degrades layer by layer, as the steps are ~2.8 nm in height.

**Table 1**

Comparison of k-values based on FT-IR and synchrotron SAXS experiments for DNA-complexes during the drying process. The FT-IR measurements allow to study the behavior of DNA and DDAB separately while SAXS measurements give information about the overall structure reception unit. The switching behavior of the DNA-DDAB complexes seem to be affected by cholesterol, but not by ethidium bromide.

	DNA-DDAB complex		Cholesterol blends	Eth. Br. Blends
	FT-IR	SAXS	FT-IR	FT-IR
<b>DNA</b>	0.017	X	0.033	0.011
<b>DDAB</b>	0.011	X	0.033	0.01
<b>complex</b>	X	0.008	X	X